



## SHORTCOMINGS OF THE ASCE 43-05 APPROXIMATE METHOD FOR ESTIMATING THE SEISMIC DEMANDS ON ROCKING OBJECTS IN CANADIAN NUCLEAR POWER PLANTS

### Amitabh Dar

Technical Advisor, Bruce Power, Canada  
Doctoral Researcher, McMaster University  
[dara@mcmaster.ca](mailto:dara@mcmaster.ca)

### Dimitrios Konstantinidis

Assistant Professor, McMaster University  
[konstant@mcmaster.ca](mailto:konstant@mcmaster.ca)

### Wael W. El-Dakhakhni

Associate Professor, McMaster University  
[eldak@mcmaster.ca](mailto:eldak@mcmaster.ca)

**ABSTRACT:** Within a nuclear power plant, there is a multitude of components, such as portable standby generators, small portable transformers, tool cabinets, carts, etc., that cannot be anchored to a fixed location due to the need for frequent movement. During earthquake shaking, such components may slide, rock, and possibly overturn. The seismic interaction of an unanchored object with a safety system or component may lead to serious consequences. Canadian nuclear standards do not provide any seismic criteria for rocking objects, and there is very limited guidance available in the nuclear industry except for an approximate method given in ASCE 43-05 to estimate the maximum rotation of a rocking object. This method considers a rocking block as an equivalent viscously damped linear single-degree-of-freedom (SDOF) oscillator. This paper compares the peak response of a rocking block as estimated by the ASCE 43-05 method, applied to the Canadian generic response spectrum given in the Canadian standard CSA N289.3, with the peak response obtained by directly solving the nonlinear equations of motion of a rocking block. The paper concludes that the approximate method in ASCE 43-05 provides a poor approximation for the peak rotation angle of a rocking object in a nuclear power plant.

### 1. Introduction

The seismic design basis of a Canadian Nuclear Power Plant (NPP) is defined as the Design Basis Earthquake (DBE) represented by a corresponding response spectrum (Dar et al., 2014). The DBE of some of the relatively older Canadian plants is based on the response spectrum given by Newmark, Blume and Kapur (1973), known as the NBK spectrum. The DBE of some newer Canadian NPPs is derived by scaling the generic response spectrum specified in the CSA N289.3 standard (1981, 2010) based on the spectral shape given by Newmark and Hall (1978). Existing Canadian NPPs are required to assess the seismic risk in accordance with the Canadian Nuclear Safety Commission Regulatory Standard REGDOC 2.4.2 (CNSC, 2005) on a periodic basis. Seismic risk depends on fragilities of a host of systems and components in a NPP. While conservatism in design augments redundancy, applying it to risk analysis lowers fragilities resulting in high risk. This *artificially* amplified risk leads to the diversion of financial and technical resources of a NPP from high risk components to low risk ones.

Some of the safety components in a NPP, such as portable power supply units and power generators, require frequent movement and hence cannot be anchored, resulting in vulnerability to rocking and overturning in a seismic event. Seismic interaction of unanchored objects such as carts, scaffolding, tool

cabinets, etc., with a nearby seismically qualified system or component can be detrimental to nuclear safety. While there is no guidance given in the Canadian nuclear standards on how to deal with rocking objects, the ASCE 43-05 (2005) standard allows unanchored components inside a NPP as long as they meet certain seismic design criteria. The relevant criteria in ASCE 43-05 are based on an approximate method of estimating the peak rocking rotation of unanchored objects under the assumption that they can be represented by equivalent SDOF oscillators.

An unanchored rigid block subject to base excitation may slide, rock or slide-rock. Shenton (1996) established the criteria of initiation of these three modes of response. The response of sliding objects to base excitation has been studied by Shao and Tung (1999) Choi and Tung (2002), Lopez and Soong (2003), Comerio (2005), Konstantinidis and Makris (2009; 2010), Konstantinidis and Nikfar (2015), Lin et al. (2015), and references given therein. The problem of pure planar rocking of single blocks or block assemblages has been investigated at various levels by Housner (1963), Yim et al. (1980), Makris and Roussos (2000), Zhang and Makris (2001), Konstantinidis and Makris (2005a; 2005b), Makris and Vassiliou (2013), and reference reported therein.

ASCE 43-05 permits the consideration of rocking and sliding responses separately, and for rocking it focuses on pure planar response. The attempt to derive the rocking response of a rigid block by considering it equivalent to a SDOF oscillator by Priestley et al. (1978) was challenged by Makris and Konstantinidis (2003), who demonstrated that this approach leads to an erroneous solution. A preliminary investigation of the methodology by Wesley et al. (1980), also based on an equivalent SDOF oscillator, was carried out by Dar et al. (2013) highlighting the deficiencies of this approach. Despite the strong evidence available in the literature contrary to the fundamental assumption in the ASCE 43-05 method, it continues to be utilized in the nuclear industry (Dar et al., 2015) and elsewhere. FEMA P-58-1, prepared by the Applied Technology Council (2012), has adapted this method, and the standard ASCE 4 is expected to include it in its new revision (Jensen and Gurbuz, 2011). Dar et al. (2015) have carried out a detailed evaluation of the ASCE 43-05 method by uncovering its inherent problems and concluding that the rocking response obtained by non-linear analysis is much more reliable, accurate and less time consuming than the response obtained by following the ASCE 43-05 method. The differences between the ASCE 43-05 approach and the methodology by Priestley et al. (1978) have been highlighted by Dar et al. (2015).

This paper highlights the shortcomings of the ASCE 43-05 approach by comparing its predictions against the results of full nonlinear analysis (NLA) of a rocking block subjected to selected earthquake records. The example given in ASCE 43-05 incorporates pure planar rocking response and hence the same is considered in this paper. Since the ASCE 43-05 method is based on a response spectrum, the generic spectrum recommended for the Canadian NPPs by CSA N289.3 (2010) is considered.

## 2. Review of Rigid Rocking Block

Figure 1(a) shows the details of a rigid block in pure planar rocking motion. The equation of motion of this rocking block is (Yim et al., 1980):

$$I_o \ddot{\theta} + mgR \sin(-\alpha - \theta) = -m\ddot{x}R \cos(-\alpha - \theta), \quad \theta < 0 \quad (1)$$

$$I_o \ddot{\theta} + mgR \sin(\alpha - \theta) = -m\ddot{x}R \cos(\alpha - \theta), \quad \theta \geq 0 \quad (2)$$

where,  $\ddot{x}$  is the base acceleration  $m$  is the mass of the block,  $R$  is the distance from the pivot point to the center of gravity, angle  $\alpha$  is the measure of block stockiness,  $g$  is the acceleration of gravity, and  $I_o$  is the mass moment of inertia of the rigid block about pivot point O. Substituting  $I_o = (4/3)mR^2$  for a rectangular block gives

$$\ddot{\theta} = -p^2 \left\{ \sin[\alpha \operatorname{sgn}(\theta) - \theta] + \frac{\ddot{x}}{g} \cos[\alpha \operatorname{sgn}(\theta) - \theta] \right\} \quad (3)$$

where  $p = \sqrt{3g/(4R)}$ , the so-called frequency parameter and  $\operatorname{sgn}(\cdot)$  is the *signum* function.

Eq. 3 can be solved numerically by employing a state space formulation (Makris and Konstantinidis, 2003). The energy loss due to impact is accounted for by obtaining the post-impact velocity  $\dot{\theta}_2$  by multiplying the pre-impact velocity  $\dot{\theta}_1$  by the maximum coefficient of restitution, given by Housner (1963),

$$r = 1 - \frac{3}{2} \sin^2 \alpha \quad (4)$$

For slender blocks, Housner (1963) simplified the equation of motion (Eq. 3) as

$$\ddot{\theta} - p^2 \theta = -p^2 \alpha \text{ for } \theta \geq 0 \quad (5)$$

The solution for the above free vibration equation, with initial rotation  $\theta_0$ , is (Housner, 1963),

$$\theta = \alpha - (\alpha - \theta_0) \cosh(pt) \quad (6)$$

Housner (1963) obtained the time required for the block to drop from the initial rotation  $\theta_0$  to zero, which represents the quarter cycle period. Multiplying this by four and considering no energy loss due to impact, the period of free vibration, named 'Housner Period' (Dar et al., 2015), denoted by  $T_H$ , is given as

$$T_H = \frac{4}{p} \cosh^{-1} \left[ \frac{1}{1 - \left( \frac{\theta_0}{\alpha} \right)} \right] \quad (7)$$

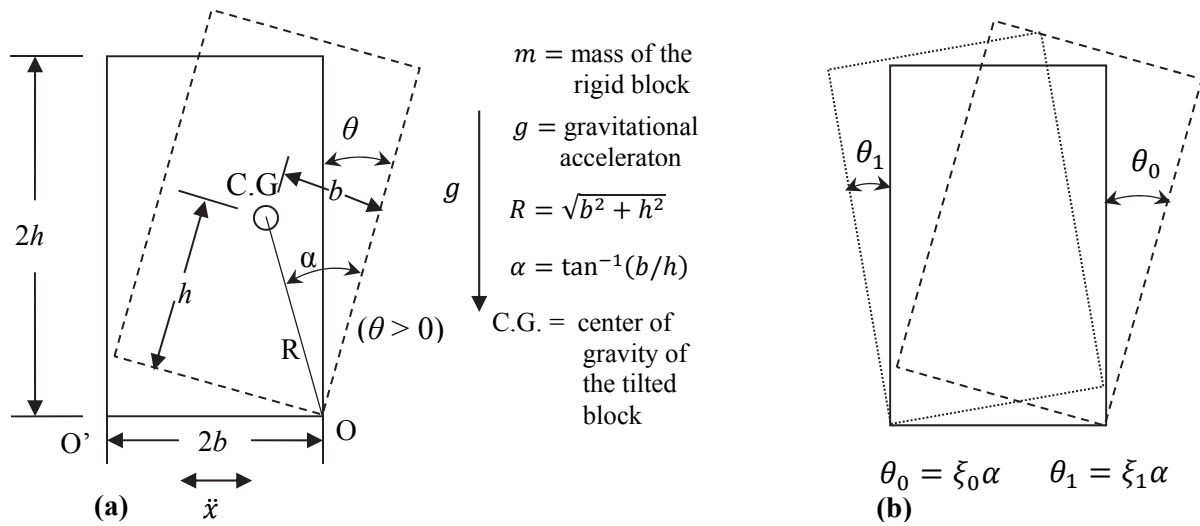


**Fig. 1 – (a) Rigid rocking block in rocking motion (b) Peak rotation after impact in free vibration**

For free vibration condition, as shown in Fig. 1(b), for initial rotation  $\theta_0 = \xi_0 \alpha$  at  $t = 0$ , the peak rotation after the first impact is  $\theta_1 = \xi_1 \alpha$ , where  $\xi_1$  is obtained from Eq. 5 and 6 as,

$$\xi_1 = 1 - \sqrt{\xi_0^2 r^2 - 2\xi_0 r^2 + 1} \quad (8)$$

From Eq. 8, various successive free vibration peak rotations can be found after each impact. Figure 2(a) shows quarter cycle response over normalized time  $\bar{t} = t/T_H$  by Eq. 6 for three successive peak rotations starting from  $\xi_0 = 0.99$  for the example considered in Appendix B of ASCE 43-05 given in Table 1. Figure 2(b) shows free vibration response curves without energy loss over normalized time starting with initial normalized rotations  $\xi_0$ ,  $\xi_1$  and  $\xi_2$ . The total response including the impact over normalized time  $\bar{t}$  can be obtained by considering the curve 1 for the first cycle, curve 2 for the second and so on. Figure 2(c) shows that by adding various quarter cycle response curves, total response over time can be obtained which is the same as the nonlinear solution given by solving Eq. 5 utilizing AdamsBDF hybrid solver (PTC, 2012). It is evident from Fig. 2(c) that larger peak rotation results in flatter peak indicating that for relatively larger rotations a rocking block spends much more time away from the equilibrium position (zero rotation) than close to it. Here,  $|\theta/\alpha| > 0.25$  is considered away from zero.

**Table 1 – Details of ASCE 43-05 example block**

$\alpha$	$R$ (mm)	$p$ (rad/s)	$2\pi/p$ (s)	$r$	$F_V$	$F_H$
0.405	1161	2.517	2.496	0.767	1.04	1

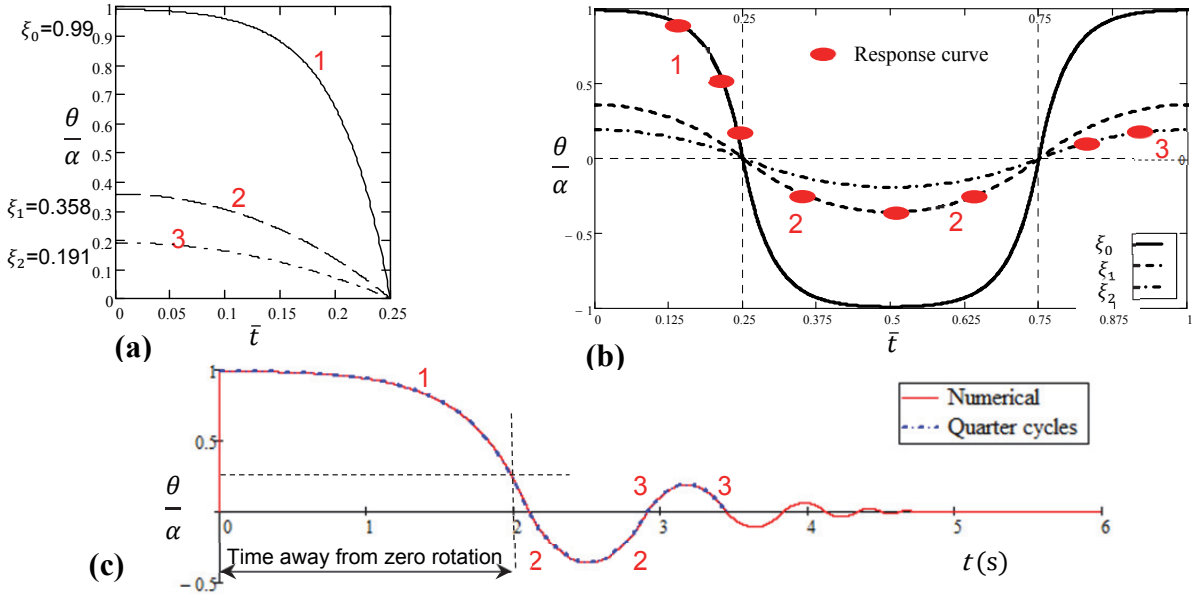


**Fig. 2 – (a) Housner's quarter cycle solutions, (b) Combination of quarter cycle solutions, (c)Comparison of Housner's solution with numerical solution (for the block in Table 1)**

### 3. ASCE 43-05 Method for Estimating Peak Rocking Rotation

The ASCE 43-05 method begins with Eq. 1 including the vertical base acceleration,  $\ddot{y}$ ,

$$I_o\ddot{\theta} + m(g + \ddot{y})R\sin(\alpha - \theta) = -mRF_H\cos(\alpha - \theta)\ddot{x} \quad (9)$$

where  $F_H$  is a dimensionless factor meant to account for non-uniform mass distribution (ASCE, 2005). For a block with uniformly distributed mass,  $F_H = 1$ . Eq. 9 can be expressed as

$$\ddot{\theta} + \frac{g}{C_I h} f_2(\theta) = \frac{-f_1(\theta)F_H\ddot{x} - f_2(\theta)\ddot{y}}{C_I h} \quad (10)$$

where  $C_I = (4/3)(1 + a^2)$ , and  $a = \tan \alpha = b/h$  (Fig. 1). Functions  $f_1(\theta)$  and  $f_2(\theta)$  are defined as

$$f_1(\theta) = \cos \theta + a \sin \theta \quad f_2(\theta) = a \cos \theta - \sin \theta \quad (11)$$

At this point, ASCE 43-05 assumes that a rocking block's nonlinear dynamical system can be represented by a linear SDOF oscillator, and the term  $(g/C_I h)f_2(\theta)$  is replaced by  $\omega_e^2\theta$ . The equivalent natural frequency  $\omega_e$  of a SDOF oscillator is obtained by equating the work required to twist a rotational spring of stiffness  $K_R$  by  $\theta_o$ , i.e.,  $= (1/2)K_R\theta_o^2$ , with the work done to rotate a block from  $\theta = 0$  to  $= \theta_o$ , giving,

$$\omega_e = \sqrt{\frac{K_R}{I_o}} = \sqrt{\frac{2[f_1(\theta_o)-1]g}{C_I \theta_o^2 h}} \quad (12)$$

ASCE 43-05 then considers the time-average values of  $f_1(\theta) \approx 1$  and  $f_2(\theta) \approx a$ , assuming that a block spends much more time near zero rotation than away from it. Thus Eq. 10 simplifies to:

$$\ddot{\theta} + \omega_e^2\theta = \frac{-F_H\ddot{x} - a\ddot{y}}{C_I h} \quad (13)$$

Assuming random phasing of the horizontal and vertical spectral accelerations,  $SAH$  and  $SAV$  with respect to each other, ASCE 43-05 obtains the horizontal acceleration capacity  $SAH_{CAP}$  from Eq. 12 and 13,

$$SAH_{CAP} = \frac{2g[f_1(\theta_o)-1]}{F_H F_V \theta_o} \quad (14)$$

where  $F_V = \sqrt{1 + [(a SAV)/(F_H SAH)]^2}$ . For  $SAV/SAH = 2/3$  (as recommended in the CSA N289.3 (2010)) spectrum,  $F_V$  has negligible impact, and according to ASCE 43-05 can be ignored. In the sequel, a uniform block (i.e.,  $F_H = 1$ ) is considered.

#### 4. ASCE 43-05 Procedure

As evident from Eq. 12, the equivalent frequency of a SDOF oscillator depends on, and is inversely proportion to, the maximum angle of rotation  $\theta_o$  of a rigid rectangular block. The spectral acceleration depends on the equivalent frequency of a SDOF oscillator, which remains unknown unless the maximum rotation  $\theta_o$  of the rigid block is known. ASCE 43-05 recommends an iterative procedure by first considering the frequency  $f_{em}$  at the peak spectral acceleration (SA) of an applicable response spectrum. From this frequency, it calculates the first value of  $\theta_o$  and defines it as the minimum of the maximum angle of rotation  $\theta_{om}$ , given below, obtained from Eq. 12 by substituting,  $f_1(\theta_o) - 1 \approx \theta_o \left( a - \frac{\theta_o}{2} \right)$ .

$$\theta_{om} = \frac{2a}{\frac{c_L}{g}(2\pi f_{em})^2 + 1} \quad (15)$$

For this angle of rotation, the horizontal acceleration capacity (from Eq. 14) is compared with the peak SA. If the capacity is equal to the peak SA then maximum rotation would be equal to  $\theta_{om}$ . Otherwise  $\theta_o$  is increased in suitable increments ( $\theta_o = \theta_{om} + \Delta\theta$ ), e.g.,  $\Delta\theta = 0.01$ . Each  $\theta_o$  leads to a corresponding angular frequency  $\omega_e$  from Eq. 12 giving  $f_e = \omega_e/2\pi$ , till  $SAH_{CAP} = SA$  at  $f_e$ . In case of two values of  $\theta_o$  satisfying the condition,  $SAH_{CAP} = SA$ , the lower value of  $\theta_o$  is considered as solution. Or, in order to simplify the above procedure, a *capacity curve* as defined by Dar et al. (2015) can be drawn, by varying  $\theta_o$  in increment of 0.001, up to  $\alpha$ . Intersection of this capacity curve with the response spectrum, closest to the peak SA is considered as solution. The capacity and frequency equations (Eq. 14 and 12 respectively) with small angle approximation, expressed in terms of  $p$  and  $\alpha$  (Dar et al., 2015), resolve to,

$$SAH_{CAP} = \alpha g \left( 2 - \frac{\theta_o}{\alpha} \right) \quad \text{and} \quad f_e = \frac{\omega_e}{2\pi} = \frac{p}{2\pi} \sqrt{\frac{2}{\frac{\theta_o}{\alpha}} - 1} \quad (16)$$

The capacity curve can be obtained from the above set of equations by varying  $\theta_o/\alpha$ , from a small value, say 0.001 to 1 with small angle approximation ( $\alpha < 0.35$ ). ASCE 43-05 assumes overturning at  $\theta_o/\alpha = 1$ . However, it is known that the overturning may occur at  $\theta_o/\alpha > 1$  in certain cases (Zhang and Makris, 2001). Figure 3(a) shows the solution for the ASCE 43-05 example (Table 1), with respect to the CSA spectrum with the equivalent frequency of a SDOF as 2.028 Hz corresponding to  $\theta_o = 0.0297$ .

#### 5. CSA Spectrum Following the ASCE 43-05 Method

The generic response spectrum given in CSA N289.3 (2010), anchored to 0.1g, is governed by control frequencies at 0.02 Hz, 0.08 Hz, 7 Hz and 33 Hz and two damping-dependent frequencies between 0.08 Hz and 7 Hz. The amplification factors for different damping values are given in CSA N289.3 (2010) which recommends scaling the generic CSA spectrum to the PGA of the site. Fig. 3(a) shows the CSA spectrum scaled to (or anchored at) 0.41g PGA at 8.4% damping computed in the manner described below. Unlike the NBK spectrum (Newmark et al., 1973) where only the amplified displacement amplitudes remains constant over a prescribed range of frequencies, the CSA spectrum defines frequency ranges for constant displacement, velocity and acceleration. ASCE 43-05 calculates damping by equating the ratio of two successive displacement amplitudes of the free vibration response of a SDOF oscillator with square (because of two impacts in one cycle) of the coefficient of restitution,

$$\frac{u_{n+1}}{u_n} = e^{-\gamma} = r^2 \quad (17)$$

where  $= 2\pi\beta_e/\sqrt{1 - \beta_e^2}$ ,  $\beta_e$  is the equivalent damping ratio, and  $r$  is given by Eq. 4. This leads to

$$\beta_e = \frac{\gamma}{\sqrt{4\pi^2 + \gamma^2}} \quad (18)$$

Where,  $\gamma = -2 \ln \left( 1 - \frac{3}{2} \sin^2 \alpha \right)$

#### 6. Inherent Problems in the ASCE 43-05 Method

Dar et al. (2015) have reported several inherent problems in the ASCE 43-05 method when applied to the NBK spectrum. Some of them are narrated below as they apply to the CSA spectrum.

- **Assumption that the rocking block can be represented by a SDOF oscillator.** The positive sign attached to the term  $(g/C_I h)f_2(\theta)$  in Eq. 10 gives the impression of a positive stiffness. However, expanding this term leads to

$$\frac{g}{C_I h}f_2(\theta) = p^2 \sin(\alpha - \theta) = p^2[\sin \alpha - (\cos \alpha) \theta + \dots] \quad (19)$$

The negative sign in front of the  $\theta$  term indicates negative stiffness, something which is clouded by the appearance of Eq. 10. The assumption that a rocking block (inverted pendulum) can be represented by a SDOF oscillator (pendulum) in the ASCE 43-05 method is fundamentally flawed.

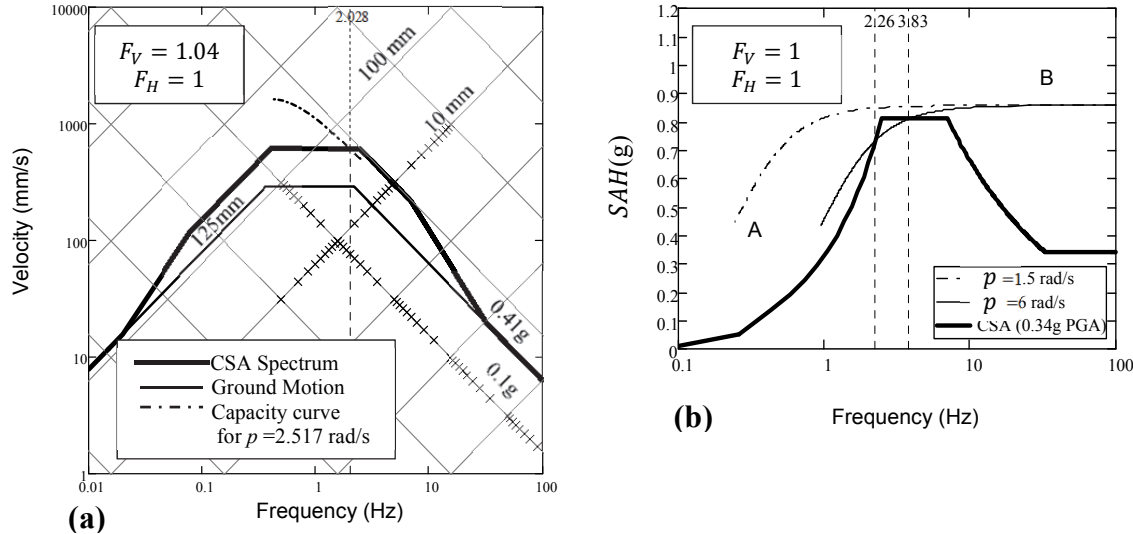


**Fig. 3 – (a) CSA spectrum (0.41g PGA, 8.4% damping) and capacity curve for the example block in Table 1, (b) Solution for two values of  $p$  with  $\alpha = 0.045 \text{ rad}$ ,  $F_H = 1$  and  $F_V = 1$ .**

- **Non-unique solution.** Figure 3(b) shows two capacity curves, for  $p = 1.5$  and  $6 \text{ rad/s}$  (both for  $\alpha = 0.405 \text{ rad}$ ) along with the CSA spectrum anchored to  $0.34g$ . While the capacity of the block with  $p = 1.5 \text{ rad/s}$  is more than the spectral accelerations over the entire range of frequencies, signifying *no rotation*, the ASCE 43-05 method for  $p = 6 \text{ rad/s}$  gives solutions at two frequencies,  $3.83$  and  $2.26 \text{ Hz}$ . This is because the CSA spectrum has a flat peak, giving a range of peak frequencies. If the largest frequency ( $7 \text{ Hz}$ ) is considered as the peak frequency, the first value of  $\theta_o$  to its left is the solution, i.e.,  $f_e = 3.83 \text{ Hz}$ . Considering the smallest peak frequency (approximately  $2.5 \text{ Hz}$ ),  $f_e = 2.26 \text{ Hz}$  is obtained as solution. In this paper, to maintain similarity with the NBK spectrum, the lower bound frequency close to  $2.5 \text{ Hz}$  is considered as the peak frequency.
- **Unconservative solution recommendation.** Considering the logic of selecting the frequency at the first values of  $\theta_o$  to the left of the peak, ASCE 43-05 intends to recommend a higher frequency (lower rotation) as the solution to the rocking problem. Considering this fact, the solution of the problem in Fig. 3(b) for  $p = 6 \text{ rad/s}$  would be  $f_e = 3.83 \text{ Hz}$ . Assuming that a rocking block can be represented by a SDOF oscillator, depending on the time history of the earthquake record, the block may in fact experience higher rotation. The ASCE 43-05 method, therefore, leads to an unconservative solution.
- **Finite rotation even for  $\text{PGA} < g \tan \alpha$ .** From Eq. 16, the minimum and maximum capacities, at  $\theta_o/\alpha = 0$  and  $1$ , come out to be  $\alpha g$  and  $2\alpha g$ , falling in zones A and B, respectively, in Fig. 3(b). In other words, the ASCE 43-05 method predicts a finite rotation even for PGA that is not potent enough to initiate rocking, i.e.,  $\tan \alpha g$ , or  $\alpha g$  for small  $\alpha$ .
- **Assumption that more time is spent near zero rotation.** As evident from Fig. 2(c), for relatively large rotation, more time is spent away from zero rotation than near it. This is contrary to the ASCE 43-05 assumptions on time average values of  $f_1(\theta) \approx 1$  and  $f_2(\theta) \approx \alpha$ , which lead to Eq. 13.

## 7. Rocking Response of a Rigid Block to Earthquake Records

Eq. 3 was solved for pure planar rocking response by utilizing the AdamsBDF hybrid solver (PTC, 2012) for the rectangular rigid blocks given in Table 2 subject to unidirectional base excitation prescribed by the earthquake records listed in Table 3. The first two records in Table 3 are from Hall et al. (1976) (referred in Newmark and Hall (1978)) and also by Newmark et al. (1973). The third record is of the classical Saguenay earthquake in Canada (Boore and Atkinson, 1992). Many inconsistencies, anomalies and contradictions in the ASCE 43-05 method are given in Dar et al. (2015) incorporating NBK spectrum. Figure 4 highlights some of them with respect to the CSA spectrum by comparing *rocking spectra* obtained by three different methods:

NLA: Nonlinear time history analysis of a rigid block subject to an earthquake record (i.e., direct integration of Eq. 3 with the constraint described by Eq. 4).

CSA code: ASCE 43-05 method applied to the CSA spectrum scaled to the PGA of the record.

RS code: ASCE 43-05 method applied to the response spectrum of the earthquake record

**Table 2 – Details of rigid block geometry**

Overshielding condition	$\theta/\alpha = 1$
Stockiness (Fig. 1)	$\alpha = 0.1; 0.2; 0.3 \text{ rad}$
Damping corresponding to $\alpha$ values	$\beta_e = 0.48\%; 1.9\%; 4.5\%$
Size (Fig. 1)	$0.186 \text{ m} < R \leq 11.92 \text{ m}$ (i.e., $1 < 2\pi/p \leq 8 \text{ s}$ )
Other parameters from ASCE 43-05	$m_L = m_H; F_H = 1; F_V = 1$

**Table 3 – Details of earthquake records**

Earthquake	Year	Station	Component	PGA (g)	Record
San Fernando, Calif.	1971	Pacoima Dam	S16°E	1.226	PCD 164*
Imperial Valley, Calif.	1940	EI Centro	EW	0.215	I-ELC270*
Saguenay, Quebec	1988	Site 7	85	0.174	S7_EN2**

\*<http://peer.berkeley.edu/smcat/> \*\*<http://www.earthquakescanada.nrcan.gc.ca>

The peak responses estimated using the ASCE 43-05 method are sometimes conservative and others unconservative. Contrary to the expectation that the CSA code curve would predict higher response than the NLA curve, in the first column of Fig. 4 (for  $\alpha = 0.1 \text{ rad}$ ), row (a), corresponding to the Pacoima Dam record, the NLA curve (which can be considered the ‘exact’ solution here) predicts larger response for the majority of the cases. For Pacoima Dam and  $\alpha = 0.1 \text{ rad}$ , the NLA curve predicts overturning (defined here as  $\theta_o/\alpha = 1$ ) for all values of  $2\pi/p$ , except for one case, whereas the RS code curve predicts that blocks with  $2\pi/p > 5 \text{ s}$  are safe. For very large blocks, i.e.,  $2\pi/p > 7 \text{ s}$ , the CSA code curve follows the same trend as the RS code curve, but the predicted response of the former is substantially larger. At  $2\pi/p = 7 \text{ s}$ , the response predicted by the RS code curve is approximately  $\theta_o/\alpha = 0.4$ , while the NLA curve predicts overturning. This is more than the factor of safety of 2 recommended by ASCE 43-05. In row (b), for  $\alpha = 0.1 \text{ rad}$ , corresponding to the EI Centro motion, the RS code is the most conservative, and the CSA code curve is the least conservative for the majority of cases. On the other hand, in row (c) of the same column, corresponding to the Saguenay motion, the CSA code curve is the most conservative, and the RS code curve is the least conservative. In this row, if the response of RS curve were amplified by the factor of safety of 2 (recommended by ASCE 43-05), it would artificially amplify the risk in a typical seismic probabilistic risk assessment analysis. The situation worsens if the factor of safety is applied to the CSA code curve where the response is more than 4 times the NLA curve between

$2\pi/p = 2$  to 4 s, which is in the range of interest for rocking objects in a NPP. The second and third columns of Fig. 4, corresponding to  $\alpha = 0.2$  and 0.3 rad respectively, the CSA curve, in general, provides conservative estimates, although in many cases these are grossly over-conservative.

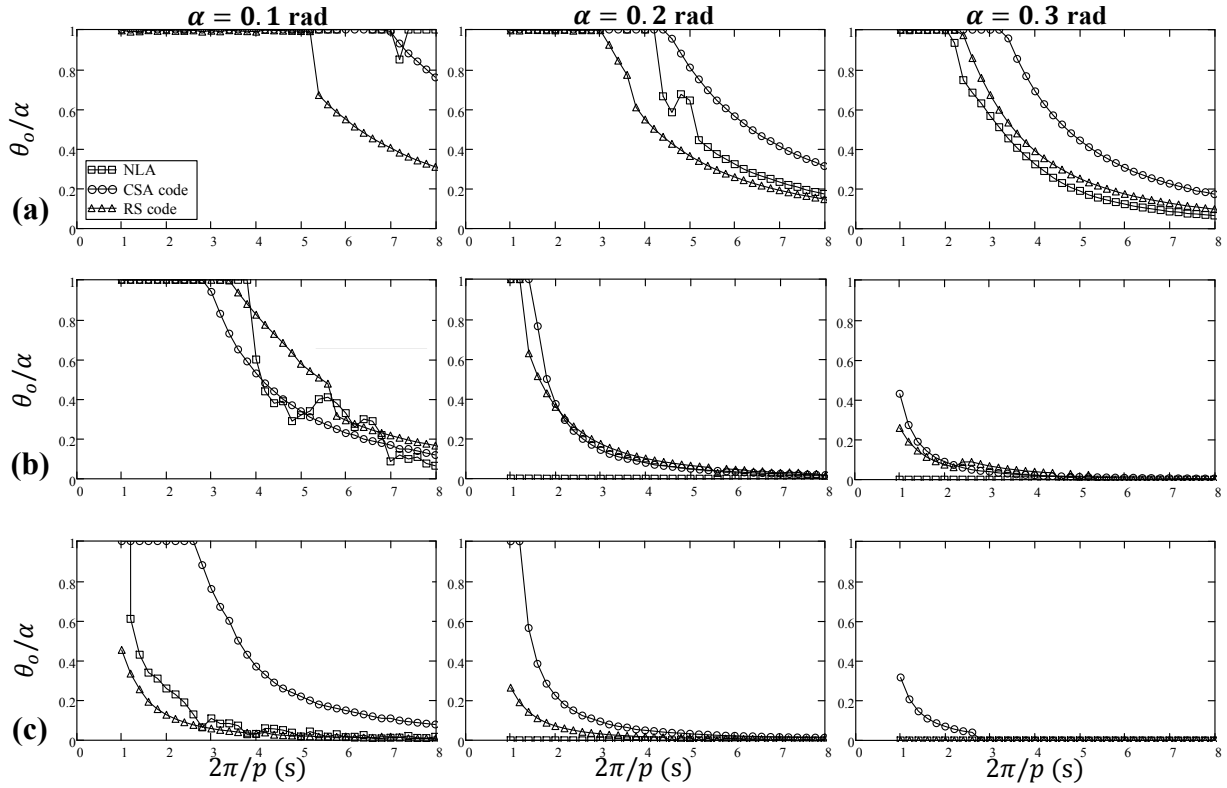


**Fig. 4 – Rocking spectra for the (a) San Fernando Pacoima Dam, (b) Imperial Valley El Centro Array #9, and (c) Saguenay Site 7 records; for three values of stockiness  $\alpha$ .**

We return now to the issue of non-unique frequency solutions provided by the ASCE 43-05 method, discussed in the previous section. Here, we seek to quantify the effect of this non-uniqueness on the peak estimated response. Figure 5(a) shows the rocking spectrum (CSA code) for  $\alpha = 0.28$  rad corresponding to the CSA spectrum anchored at 0.174g, the PGA of the Saguenay record. Since the CSA spectrum has a flat peak between frequencies of 2.59 Hz and 7 Hz (see Fig. 3), two CSA rocking spectra are plotted, one considering the lower bound (2.59 Hz) and the other considering the upper bound (7 Hz) frequency. It is noted that there is significant difference between the two curves for  $2\pi/p = 1$  to 3 s. This anomaly is observed when applying the ASCE 43-05 method to the response spectrum as well. The Saguenay response spectrum peaks at 4.6 Hz. However, since the CSA spectrum's applicable frequency is 2.5Hz, it should be applied to the response spectrum also. Considering both these frequencies as the starting points (as  $f_{em}$  in Eq. 15), two rocking spectra are plotted in Fig. 5(b) by applying the ASCE 43-05 method to the response spectrum of the Saguenay record. Figure 5(a) and (b) demonstrate that, for a response spectrum with multiple peaks or flat peak, the rocking spectra obtained by the ASCE 43-05 method leads to varying results depending on the ‘choice’ of the peak frequency.

In closing, we touch upon the level of effort associated with implementation of the ASCE 43-05 procedure. In a NPP, in-structure response spectra are created for various floor elevations. Given the absolute acceleration history of a floor, the ASCE 43-05 method requires two steps: (1) Creation of a floor response spectrum, and (2) Creation of a rocking spectrum from the floor response spectrum. On the other hand, nonlinear time history analysis of rocking block subjected to the floor motion (i.e., direct integration of Eq. 3 with the constraint described by Eq. 4) results in the rocking spectrum directly.

Despite the fact that the ASCE 43-05 method is considered approximate, the level of effort required in carrying out the procedure is significantly high compared to nonlinear time history analysis.

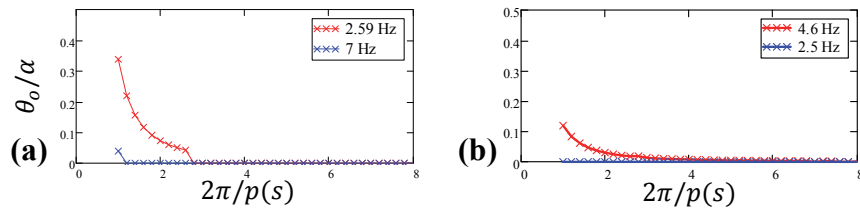


**Fig. 5 – Rocking spectra for  $\alpha = 0.28$  rad corresponding to (a) CSA spectrum anchored at 0.174g (=PGA of the Saguenay record) for two peak frequencies, and (b) Saguenay record Response spectrum based on peak frequency 4.6 Hz and 2.5 Hz**

## 8. Conclusions

It is concluded that the ASCE 43-05 method, whether applied to the scaled CSA spectrum or to the response spectrum of an earthquake record, provides inconsistent and unreliable results, which are in many cases unconservative in comparison to the nonlinear time history analysis. An approximate method is expected to be relatively simple to implement and provide reasonably conservative results. The ASCE 43-05 method, however, does not satisfy either of these basic requirements. There is evidence available in the literature challenging the validity of the fundamental assumption of the ASCE 43-05 method that the rocking response of a rigid block subject to base excitation can be obtained by an equivalent SDOF oscillator. The findings of this study confirm that this assumption is erroneous and leads to unreliable results. It is therefore recommended that the ASCE 43-05 method is not used to estimate the response of a rocking block; instead, nonlinear time history analysis should be carried out.

## 9. References

- Applied Technology Council, *Seismic Performance Assessment of Buildings FEMA P-58-1*. Washington, D.C.: Federal Emergency Management Agency, 2012.
- ASCE, *ASCE 43-05: Seismic Design Criteria for Structures, Systems and Components in Nuclear Facilities*, Reston, VA: American Society of Civil Engineers, 2005.
- Boore, D. M., and Atkinson, G. M., "Source Spectra for the 1988 Saguenay, Quebec Earthquakes". *Bulletin of the Seismological Society of America*, 82(2), 1992, 683-719.
- Choi, B., and Tung, C. D. "Estimating Sliding Displacement of an Unanchored Body Subjected to Earthquake", *Earthquake Spectra*, 18(4), 2002, 601–613.
- CNSC, *Probabilistic Safety Assessment (PSA) for Nuclear Power Plants REGDOC 2.4.2*, Canadian Nuclear Safety Commission, 2005.
- Comerio, M. C., *Testbed Study on a Laboratory Building: Exercising Seismic Performance Assessment. Report No. 2005/12*. Berkeley: Pacific Earthquake Engineering Research Center (PEER) University of California, 2005.
- CSA, *CSA N289.3. Design Procedures for Seismic Qualification of CANDU Nuclear Power Plants*. Rexdale, Ontario, Canada: Canadian Standards Association, 1981, 2010.
- Dar, A., Konstantinidis, D., El-Dakhakhni, W., "Requirement of Rocking Spectrum in Canadian Nuclear Standards", *Transactions, 22nd International Structural Mechanics in Reactor Technology Conference (SMiRT22)*, San Francisco, CA, 2013.
- Dar, A., Konstantinidis, D., El-Dakhakhni, W. W., "Evaluation of ASCE 43-05 Seismic Design Criteria for Rocking Objects in Nuclear Facilities", *Journal of Structural Engineering (under review)*, 2015.
- Hall, W. J., Mohraz, B., Newmark, N. M., *Statistical Studies of Vertical and Horizontal Earthquake Spectra NUREG-003*, United States Nuclear Regulatory Commission, 1976.
- Housner, G. W., "The Behavior of Inverted Pendulum Structures During Earthquakes", *Bulletin of the Seismological Society of America*, 53 (2), 1963, pp. 403–417..

- Jensen, S. R., Gurbuz, O., "Chapter 7.6 ASCE 4 Revision 2. : Sliding and Rocking of Unanchored Components and Structures", *Structures Congress*, Las Vegas: American Society of Civil Engineers, 2011, pp. 2178-2189..
- Konstantinidis, D., Makris, N., *Experimental and analytical studies on the seismic response of freestanding and anchored laboratory equipment*, University of California, Berkeley, Pacific Earthquake Engineering Research Center(PEER), 2005a.
- Konstantinidis, D., Makris, N., "Seismic Response Analysis of Multidrum Classical Columns", *Earthquake Engineering and Structural Dynamics*, 34(10), 2005b, pp. 1243–1270.
- Konstantinidis, D., Makris, N., "Experimental and Analytical Studies on the Response of Freestanding Laboratory Equipment to Earthquake Shaking", *Earthquake Engineering and Structural Dynamics*, 38(6), 2009, pp. 827–848.
- Konstantinidis, D., Makris, N., Experimental and Analytical Studies on the Response of 1/4-Scale Models of Freestanding Laboratory Equipment Subjected to Strong Earthquake Shaking. *Bulletin of Earthquake Engineering*, 8(6), 1457–1477, 2010.
- Konstantinidis, D., Nikfar, F., Seismic Response of Sliding Equipment and Contents in Base-isolated Buildings Subjected to Broad-band Ground Motions. *Earthquake Engineering and Structural Dynamics*, 44(6), 2015, pp. 865–887.
- Lin, S. L., MacRae, G. A., Dhakal, R. P., Yeow, T. Z., Building Contents Sliding Demands in Elastically Responding Structures. *Engineering Structures*, 86, 2015.
- Lopez, G. D., Soong, T., "Sliding Fragility of Block-type Non-structural Components. Part 1: Unrestrained Components", *Earthquake Engineering and Structural Dynamics*, 32(1), 2003, pp. 111–129.
- Makris, N., Konstantinidis, D., "The Rocking Spectrum and the Limitations of Practical Design Methodologies", *Earthquake Engineering and Structural Dynamics*, 32 (2), 2003, pp. 265–289.
- Makris, N., Roussos, Y., "Rocking response of rigid blocks under near-source ground motions", *Géotechnique*, 50(3), 2000, 243–262.
- Makris, N., Vassiliou, M., "Planar Rocking Response and Stability Analysis of an Array of Free-standing Columns Capped With a Freely Supported Rigid Beam", *Earthquake Engineering and Structural Dynamics*, 42(3), 2013, pp. 431-449.
- Newmark, N. M., Hall, W. J., *Development of criteria for seismic review of selected nuclear power plant NUREG/CR-0098*, United States Nuclear Regulatory Commission, 1978.
- Newmark, N. M., Blume, J. H., Kapur, K. K., "Seismic Design Spectra for Nuclear Power Plants", *Journal of the Power Division, ASCE*, 99(PO2), November, 1973, pp. 287-303.
- Priestley, M., Evison, R., Carr, A. J., "Seismic Response of Structures Free to Rock on Their Foundations", *Bulletin of the New Zealand National Society for Earthquake Engineering*, 11(3), 1978, pp.141–150.
- PTC, Mathcad 15.0, Parametric Technology Corporation, 140 Kendrick Street, Needham, MA 02494, USA, 2012.
- Shao, Y., Tung, C., "Seismic Response of Unanchored Bodies", *Earthquake Spectra*, 15(3), 1999, pp. 523–536.
- Shenton III, H. W., "Criteria for Initiation of Slide, Rock, and Slide-Rock Rigid-Body Modes", *Journal of Engineering Mechanics (ASCE)*, 122 (7), 1996, pp. 690–693.
- Wesley, D. A., Kennedy, R. P., Richter, P. J., "Analysis of the Seismic Collapse Capacity of Unreinforced Masonry Wall Structures", *Proc. 7th World Conference on Earthquake Engineering*. Istanbul, Turkey, 1980.
- Yim, C. K., Chopra, A., Penzien, J., "Rocking Response of Rigid Blocks to Earthquakes", *Earthquake Engineering and Structural Dynamics*, 8(6), 1980, pp. 565–587.
- Zhang, J., Makris, N., "Rocking Response of Free-Standing Blocks Under Cycloidal Pulses", *Journal of Engineering Mechanics (ASCE)*, 127(5), 2001, 473-483.